



Missouri University of Science and Technology
Scholars' Mine

International Specialty Conference on Cold-Formed Steel Structures

Wei-Wen Yu International Specialty Conference on Cold-Formed Steel Structures 2016

Nov 9th, 12:00 AM - 12:00 AM

Distortional Buckling Experiment on Cold-Formed Steel Lipped Channel Columns with Circle Holes under Axial Compression

Xingyou Yao

Yanli Guo

Zhen Nie

Follow this and additional works at: <https://scholarsmine.mst.edu/isccss>

 Part of the [Structural Engineering Commons](#)

Recommended Citation

Yao, Xingyou; Guo, Yanli; and Nie, Zhen, "Distortional Buckling Experiment on Cold-Formed Steel Lipped Channel Columns with Circle Holes under Axial Compression" (2016). *International Specialty Conference on Cold-Formed Steel Structures*. 6.

<https://scholarsmine.mst.edu/isccss/23iccfss/session2/6>

This Article - Conference proceedings is brought to you for free and open access by Scholars' Mine. It has been accepted for inclusion in International Specialty Conference on Cold-Formed Steel Structures by an authorized administrator of Scholars' Mine. This work is protected by U. S. Copyright Law. Unauthorized use including reproduction for redistribution requires the permission of the copyright holder. For more information, please contact scholarsmine@mst.edu.

Distortional Buckling Experiment on Cold-formed Steel Lipped Channel Columns with Circle Holes under Axial Compression

YAO Xingyou^{1,2}, GUO Yanli³, NIE Zhen⁴

Abstract

The objective of this paper is to research the distortional buckling mode and load-carrying capacity of cold-formed thin-walled steel columns with circle holes in web. Compression tests were conducted on 26 intermediate length columns with and without holes. The test members included four different kinds of circle holes. Test results show that the distortional buckling occurred for intermediate columns with holes and the strength of columns with holes was less than that of columns without circle hole. The ultimate strength of columns decreased with the increase of the total transverse width of hole in cross-section of members. For each specimen, a shell finite element Eigen-buckling analysis and nonlinear analysis was also conducted. Analysis results show that the holes can affect on the elastic buckling stress of columns. The shell finite element can be used to model the buckling modes of columns with holes and analyze the load-carrying capacities of members with holes. The comparison on ultimate strength between test results and calculated results using Chinese code GB50018-2002, *North American specification* AISI S100-2016 and nonlinear Finite Element method was made. The calculated ultimate strength show that results predicted with AISI S100-2016 and analyzed using finite element method are close to test results. The calculated results using Chinese code is higher than test results because Chinese code has no provision to calculate the ultimate strength of members with holes. So the calculated method for cold-formed steel columns with circle holes was proposed. The calculated results using this proposed method show good agreement with test results and can be used in engineering design of cold-formed steel columns with circle hole.

¹ Assistant Professor, Nanchang Institute of Technology, Nanchang ,China

² Post Doctor, Tongji University, Shanghai, China

³ Assistant Professor, Nanchang Institute of Technology, Nanchang ,China

⁴ Doctor student, Tongji University, Shanghai, China

Introduction

Cold-formed steel structural sections used in the walls of residential buildings and agricultural facilities are commonly C-shape sections with holes in web. These holes located in the web of sections can alter the elastic stiffness and ultimate strength of a structural member (Moen, 2008). The stud columns with holes tests were conducted (Abdel-Rahman, 1997; Banwait,1987; Looove,1984; Ortiz-Colberg,1981; Pu, Godley, and Beale, et al, 1999; Rhodes and Schneider, 1994; Sivakumaran,1987) and the type, location, and dimension of hole were taken into account. Based on these studies, the design method for the ultimate strength of members with holes was developed considering local buckling and yielding strength. This design method is used in North American cold-formed steel specification (AISI-S100-2016, 2016). In recent years, the elastic buckling performance and Direct Strength Method(DSM) of short and intermediate length columns with holes were studied (Moen,2008;Moen and Schafer,2008; Moen and Schafer,2009a; Moen and Schafer,2009b; Moen and Schafer,2011). These researches indicated that the web holes may modify the local and distortional elastic buckling half-wavelengths, change the critical elastic buckling loads, and decrease the post-peak ductility in some cases. Then the DSM for members with holes was put forward. The analysis (He and Zhou, 2005) demonstrated that the ultimate strength would decrease if the hole was in the range of effective width of the element. The equivalent modulus method was developed to predict the critical buckling stress of axially compressive columns with holes in web and flanges (Zhou and Yu, 2010). An equivalent volume method was proposed to consider the effect of holes based on test and analysis (Wen, 1996). While these researches did not develop a reasonable calculated method in consistent with Chinese cold-formed steel specification *Technical code of cold-formed thin-wall steel structures* (GB50018-2002, 2002) to predict the ultimate strength of cold-formed steel members with holes.

The aim of this experiment is to expand the existing columns data, especially to columns with multi-holes in web. The buckling mode and ultimate capacity are analyzed using Finite Element Method. The proposed design method of the ultimate strength for this kind of members is put forward based on Chinese cold-formed steel specification.

Experimental setup and test specimens

Test set-up

Twenty-six cold-formed steel lipped channel columns with and without circle web holes were tested to failure. The main experimental parameters are the holes type and the presence or absence of circle web holes. The

specimen naming convention is defined as AC-12-CH-1, where AC means axially-compressive members, 12 means the holes type as two holes in one row, CH means circle hole, and 1 is the repeated number of specimens.

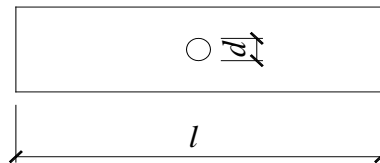
The columns compression tests are performed with 200kN capacity loaded machine shown in Fig.1. The column specimens bear directly the steel plates. Position transducers are used to measure the mid-height lateral flange displacement and vertical displacement of specimens under load.



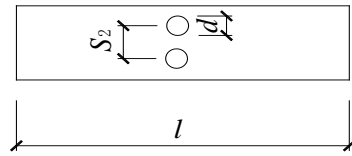
Fig. 1 Overall view of test setup

Hole type and locations

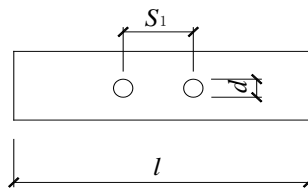
The four kinds of circle hole types (Fig.2) are selected to test and all holes are in the web of the axially compressive members, where the location of holes for the specimens with one row holes is at the mid-height of the columns, and the location of holes for the specimens with two rows holes is at the 1/3 and 2/3 height of the columns. The nominal diameter (d) of the circle hole is 14mm. The nominal transverse (S_2) and vertical (S_1) distance of holes are 50 and 250mm.



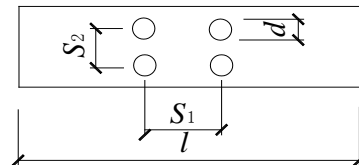
(a) One hole in one row



(b) Two holes in one row



(c) Two holes in one column



(d) Four holes in two rows and two columns

Fig.2 Holes type of the web for specimens

Section dimensions

The dimensions reference system and nomenclature for each specimen is presented in Fig.3, and the measured value was recorded at 1/4 and 1/2 points for every specimens, for a total of three measurement location for each specimens. Mean measured specimen dimensions are summarized in Table 1. The inside bend radius of specimens is $2t$, where t is the base thickness of members. l is the length of columns.

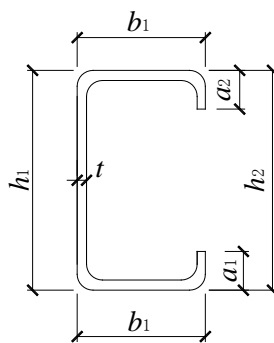


Fig. 3 Specimen measurement nomenclature

Table 1 Summary of measured specimen cross-section dimensions

| Specimens | l /mm | h_1 /mm | h_2 /mm | b_1 /mm | b_2 /mm | a_1 /mm | a_2 /mm | d /mm | t /mm | f_y /MPa |
|------------|---------|-----------|-----------|-----------|-----------|-----------|-----------|------------|------------|------------|
| AC-11-CH-1 | 800.00 | 99.45 | 99.61 | 37.66 | 38.24 | 12.05 | 12.54 | 13.93 | 1.51 | 295 |
| AC-11-CH-2 | 799.00 | 98.96 | 99.25 | 37.62 | 38.30 | 11.67 | 12.62 | 14.02 | 1.46 | 295 |
| AC-11-CH-3 | 801.00 | 99.39 | 99.53 | 37.53 | 37.94 | 12.08 | 12.40 | 13.89 | 1.49 | 295 |
| AC-11-CH-4 | 807.00 | 99.23 | 98.95 | 37.47 | 38.00 | 12.39 | 11.90 | 13.96 | 1.46 | 295 |
| AC-11-CH-5 | 800.00 | 99.13 | 99.10 | 37.81 | 38.06 | 11.87 | 12.68 | 13.88 | 1.47 | 295 |
| AC-11-CH-6 | 801.00 | 99.30 | 99.22 | 37.51 | 37.80 | 12.75 | 11.83 | 13.90 | 1.47 | 295 |
| AC-21-CH-1 | 800.00 | 100.38 | 101.74 | 37.34 | 37.11 | 12.30 | 12.28 | 14.02 | 1.45 | 295 |
| AC-21-CH-2 | 806.00 | 98.85 | 98.81 | 37.79 | 38.27 | 11.83 | 12.50 | 14.03 | 1.48 | 295 |
| AC-21-CH-3 | 799.00 | 99.27 | 98.91 | 38.15 | 37.66 | 12.35 | 11.96 | 13.92 | 1.51 | 295 |
| AC-21-CH-4 | 803.00 | 99.68 | 99.17 | 38.28 | 37.52 | 12.66 | 11.65 | 13.91 | 1.48 | 295 |
| AC-21-CH-5 | 797.00 | 99.13 | 99.33 | 38.28 | 37.55 | 13.65 | 12.03 | 13.99 | 1.47 | 295 |
| AC-21-CH-6 | 797.00 | 98.98 | 99.07 | 38.13 | 37.62 | 12.49 | 11.47 | 13.95 | 1.46 | 295 |
| AC-12-CH-1 | 802.00 | 99.39 | 99.29 | 38.95 | 37.38 | 12.70 | 12.65 | 13.97 | 1.47 | 295 |
| AC-12-CH-2 | 801.00 | 99.46 | 99.48 | 37.57 | 36.84 | 12.77 | 12.44 | 14.56 | 1.45 | 295 |
| AC-12-CH-3 | 805.00 | 99.48 | 99.46 | 37.55 | 37.22 | 12.41 | 12.53 | 12.70 | 1.49 | 295 |
| AC-12-CH-4 | 806.00 | 99.99 | 99.85 | 37.35 | 37.62 | 12.64 | 12.64 | 14.32 | 1.4 | 295 |
| AC-12-CH-5 | 803.00 | 99.78 | 99.73 | 37.40 | 37.47 | 12.71 | 11.89 | 13.28 | 1.43 | 295 |
| AC-12-CH-6 | 802.00 | 99.62 | 99.69 | 38.00 | 37.35 | 12.92 | 12.09 | 13.69 | 1.48 | 295 |
| AC-22-CH-1 | 800.00 | 99.33 | 99.82 | 37.55 | 37.63 | 12.39 | 12.33 | 13.72 | 1.44 | 295 |
| AC-22-CH-2 | 797.00 | 99.35 | 99.69 | 38.07 | 37.58 | 12.49 | 12.07 | 13.06 | 1.40 | 295 |
| AC-22-CH-3 | 789.00 | 100.38 | 100.45 | 37.65 | 38.24 | 11.24 | 13.21 | 13.61 | 1.46 | 295 |
| AC-22-CH-4 | 799.00 | 99.75 | 99.37 | 37.94 | 38.13 | 10.09 | 13.80 | 13.60 | 1.50 | 295 |
| AC-22-CH-5 | 803.00 | 99.39 | 99.09 | 37.71 | 38.20 | 10.72 | 14.29 | 12.70 | 1.39 | 295 |
| AC-22-CH-6 | 792.00 | 99.81 | 99.76 | 38.01 | 37.97 | 13.54 | 10.25 | 13.35 | 1.49 | 295 |
| AC-00-NH-1 | 802.00 | 99.87 | 99.85 | 38.22 | 37.59 | 12.39 | 13.16 | / | 1.47 | 295 |
| AC-00-NH-2 | 800.00 | 99.78 | 99.84 | 38.17 | 37.31 | 13.44 | 11.75 | / | 1.46 | 295 |

Material properties

Tension tests were carried out following the provisions of Metallic materials--Tensile testing--Part 1: Method of test at room temperature

(GB/T228.1-2010, 2010). Six tensile coupons were taken from two ends of a test member including the web flat and two flanges flat. A 200kN capacity testing machine was used for the loading. The mean values of six coupon test results are summarized. The specimen yield stress, f_y , is 295MPa reported in Table 1, the steel elastic modulus, E , is assumed as 2.074×10^5 Mpa, and the specimens elongation is 32%.

Experimental results

The failure modes of the specimens are depicted in Fig.4-Fig.6. All columns exhibit the local buckling of the web near the supports (Fig.4), one distortional half-wave buckling along the length (Fig.5), and the global flexural buckling (Fig.6) after the peak load.

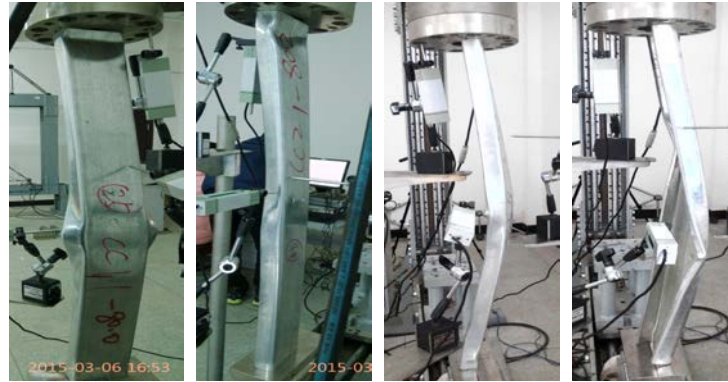


Fig.4 Local buckling mode



(a) One hole in one row (b) Two holes in one row
(c) Two holes in one column (d) Four holes in two rows and two columns

Fig.5 Distortional buckling mode



(a) One hole in one row (b) Two holes in one row
 (c) Two holes in one column (d) Four holes in two rows and two columns
 Fig.6 Global flexural buckling mode

The ultimate tested compressive load for all specimens and an average ultimate load for each test group are provided in Table 2. The circle hole are shown to have a little influence on compressive load for specimens with one hole in one row and two holes in one column, with the reduction being 6.08% and 6.28%, respectively. However, the reduction ups to 9.68% and 14.06% for the specimens with two holes in one row and four holes in two columns, respectively. These test results indicate that the circle holes have a significant influence on compressive load when the circle hole is located in the range of effective width of the web.

Table 2 Comparison on ultimate capacity of specimens

| Specimens | P_t /kN | Statistic analysis of P_t | |
|------------|-----------|-----------------------------|----------------|
| | | Mean value/kN | Hole influence |
| AC-11-CH-1 | 57.75 | | |
| AC-11-CH-2 | 60.30 | | |
| AC-11-CH-3 | 58.65 | 56.97 | 6.08% |
| AC-11-CH-4 | 57.95 | | |
| AC-11-CH-5 | 54.05 | | |
| AC-11-CH-6 | 53.10 | | |
| AC-21-CH-1 | 55.60 | | |
| AC-21-CH-2 | 57.40 | | |
| AC-21-CH-3 | 56.55 | 56.84 | 6.28% |
| AC-21-CH-4 | 57.31 | | |
| AC-21-CH-5 | 57.65 | | |
| AC-21-CH-6 | 56.55 | | |
| AC-12-CH-1 | 54.90 | 54.78 | 9.68% |
| AC-12-CH-2 | 53.65 | | |

| | | | |
|------------|-------|-------|--------|
| AC-12-CH-3 | 57.65 | | |
| AC-12-CH-4 | 55.55 | | |
| AC-12-CH-5 | 52.05 | | |
| AC-12-CH-6 | 54.90 | | |
| AC-22-CH-1 | 54.00 | | |
| AC-22-CH-2 | 52.40 | | |
| AC-22-CH-3 | 54.00 | | |
| AC-22-CH-4 | 52.05 | 52.13 | 14.06% |
| AC-22-CH-5 | 50.65 | | |
| AC-22-CH-6 | 49.65 | | |
| AC-00-NH-1 | 61.03 | | |
| AC-00-NH-2 | 60.28 | 60.66 | / |

4 Finite element analysis

Finite element model

The thin shell finite element non-linear analysis in ABAQUS was employed to simulate the experimental behavior of lipped channel compressive members with holes.

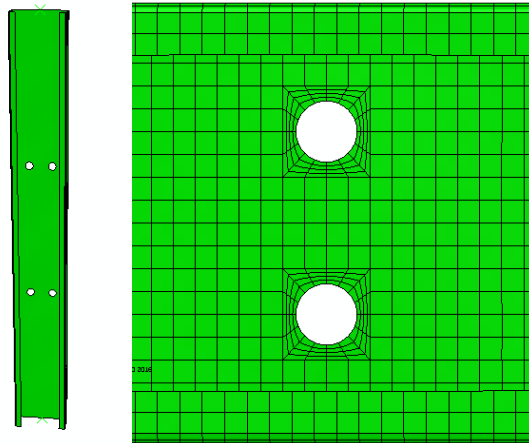
The material model was based directly on the coupon tests. The ideal elastic-plastic curve was used based on the experimental steel elastic modular and yield stress for simplifying finite element analysis. Residual stresses, residual strains and cold-work of forming effects were not included in the finite element model.

The ABAQUS S9R5 thin shell element was adopted for modeling compressive members. The mesh density was examined for stability and convergence, primarily by considering the impact of the element aspect ratio. The aspect ratio was kept below 2:1 for lips, flange, web, and corners along the length direction. In the cross-section, for the flange, web, lip, and corner, a minimum of 6, 18, 2, and 2 elements, respectively, were found to be sufficient.

The ABAQUS solution control employed was the modified Riks method and arc length method was used to ensure a stable numerical solution. All tolerances were left at the default, but initial and maximum step sizes were modified to insure repeatable and consistent results.

Imperfection sensitivity was considered in the finite element analysis. The magnitudes of the geometric imperfections adopted were $L/750$ according to Chinese cold-formed steel specification. The shape of the geometric imperfection was obtained from the first buckling mode shape of a finite

element Eigen buckling analysis in ABAQUS. The loading and boundary conditions used in the finite element analysis referred to the reference (Moen, 2008). The finite element model for specimen and the mesh of the holes are depicted in Fig.7.



(a) Columns model (b) Mesh of holes

Fig.7 Finite element model

Elastic buckling analysis

The critical elastic local buckling load (P_{cr1}), distortional buckling load (P_{crd}), and yield strength (P_y) are provided in table 3 for compressive columns with different holes type and without holes. The nominal dimensions are used in the Eigen-value elastic buckling analysis.

The comparison in Table 3 illustrates that the holes in specimens have a little effect on elastic local and distortional strength, but the effect is not significant because the ratio of the diameter of hole to the width of web is approximate 0.14.

Table 3 Comparison on critical elastic buckling loads

| Hole type | P_y /kN | P_{cr1} /kN | P_{crd} /kN |
|-----------|-----------|---------------|---------------|
| AC-11-CH | 88.5 | 69.03 | 93.68 |
| AC-21-CH | 88.5 | 68.30 | 93.24 |
| AC-12-CH | 88.5 | 68.65 | 92.88 |
| AC-22-CH | 88.5 | 67.92 | 92.97 |
| AC-00-NH | 88.5 | 71.23 | 95.29 |

The first local buckling and distortional buckling shapes for compressive

columns with different holes type and without holes are compared in Fig.8 and Fig.9.

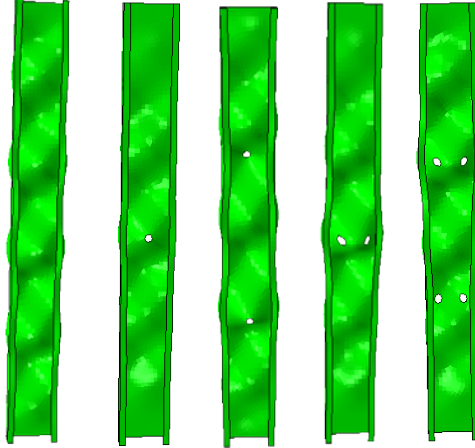


Fig.8 Comparison on local buckling mode

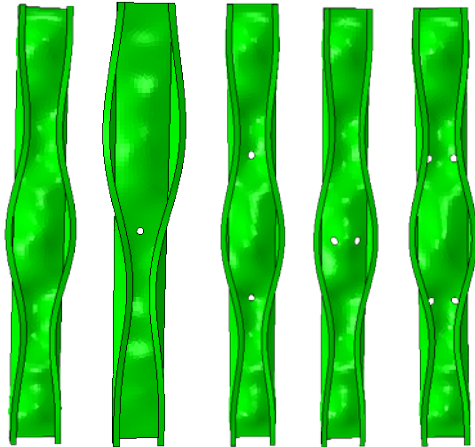


Fig.9 Comparison on distortional buckling mode

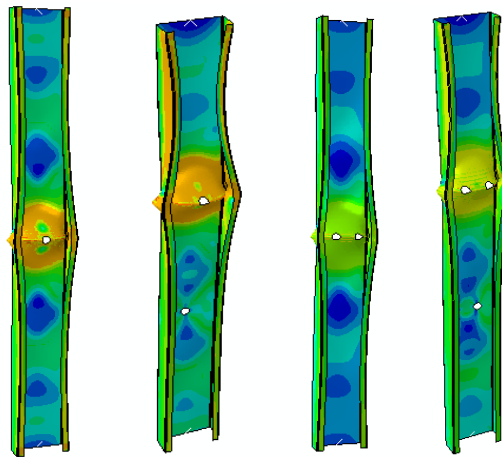
The comparison in Fig.8 and Fig.9 illustrates that the holes in specimens have no significant effect on elastic local and distortional mode when the ratio of the diameter of hole is very small.

Failure mode and capacity

The deformed shapes for the typical specimens obtained from the FEM analysis are presented in Figs. 10, which is agree to the test failure mode

depicted in Fig.4 and Fig.5. The local and distortional buckling occurs for the columns with holes. This observation suggests that the FE model can well model the buckling mode of columns with holes.

The ultimate compressive capacities (P_{ABA}) obtained from the FEM are compared with the experimental ultimate capacities (P_t) as shown in Tables 4 for each specimen. The mean values of the FEM-to-experimental ultimate compressive capacities ratio are 1.0237 with the corresponding coefficient of variation of 0.0197 for all compressive specimens. The comparison of ultimate capacity demonstrates that the ultimate compressive capacity obtained from the FEM is close to the experimental ultimate capacity and the FE model can also predict the ultimate compressive capacity well.



(a) One hole in one row (b) Two holes in one row
(c) Two holes in one column (d) Four holes in two rows and two columns
Fig.10 Failure mode of columns with holes

Proposed design method

Comparison on ultimate capacity

Two calculated method are used to predict the ultimate capacity of each specimens and evaluate every design method: (1) The Chinese cold-formed steel specification GB5018-2002, (2) The North America cold-formed steel specification AISI-S100 (2016).

The ultimate capacity of every specimen calculated using Chinese cold-formed steel specification, North America cold-formed steel specification are provided in Table 4, respectively, including ratios of predicted-to-test capacities of each specimen for two design methods,

Where P_{CI} and P_C are the ultimate capacity predicted using Chinese cold-formed steel specification with considering interaction of the elements and without considering interaction of the elements, P_N is the calculated results using North America cold-formed steel specification.

The mean values of the ratios of calculated compressive capacities to test results P_{CI} and P_C obtained using Chinese specification with considering interaction of the elements and without considering interaction of the elements is 1.0275 and 1.0702, respectively. The comparison results indicate that the current Chinese cold-formed steel specification is not safe to predict the compressive capacity of columns with holes because the code doesn't consider the effect of the holes. So the proposed method for predicting the ultimate capacity of compressive columns with holes should be analyzed and put forward based on Chinese cold-formed steel specification.

However the mean value of the ratios of calculated compressive capacities to test results using North America cold-formed steel specification is 0.9258 with the corresponding coefficient of variation of 0.0485 for columns with holes. The comparison demonstrates that North America cold-formed steel specification takes into account the effect of holes well and is conservative.

Proposed design method

The model proposal should be investigated based on the existing EWM in Chinese cold-formed steel specification in order to consider the reduction of capacity because of the affect of holes in web of compressive columns.

The effect width of the web with holes proposed for Chinese cold-formed steel specification can be determined using expression (1) based on the EWM expression of Chinese cold-formed steel specification and calculated method for the effective width of the element with circle holes in North America cold-formed steel specification when the compressive strength of columns with the holes are calculated.

$$\left\{ \begin{array}{ll} \frac{b_e}{t} = \frac{b_c - d}{t} & \frac{b}{t} \leq 18\alpha\rho \\ \frac{b_e}{t} = \left(\sqrt{\frac{21.8\alpha\rho}{\frac{b}{t}} - 0.1} \right) \frac{b_c}{t} \left(1 - \left(\frac{0.01b}{t} + 0.82 \right) \frac{d}{b_c} \right) & 18\alpha\rho < \frac{b}{t} < 38\alpha\rho \\ \frac{b_e}{t} = \frac{25\alpha\rho}{\frac{b}{t}} \frac{b_c}{t} \left(1 - \frac{1.2d}{b_c} \right) & \frac{b}{t} \geq 38\alpha\rho \end{array} \right. \quad (1)$$

where b and t are the width and thickness of the element in question, respectively; d is the diameter of circle hole; b_e is the effective width; α is a coefficient, and $\alpha=1.15-0.15\psi$, or equal to 1.15 if $\psi<0$; ψ is an uneven coefficient of the compression stress distribution (for axially-compressive members, $\psi=1$); b_c is the compressive width of the plate; ρ is a calculating coefficient, $\rho = \sqrt{235kk_1/f_y}$; k is the stability coefficient of the element under compression; k_1 is the interaction coefficient due to the adjacent element. If the interaction of the elements is not considered, $k_1=1$.

Meanwhile, the calculated effective width of web with holes should be less than the net section width of web.

The compressive capacities of each specimen calculated using proposed method are provided in Table 4. P_{S1} and P_{S2} are the compressive capacity calculated using proposed method with considering interaction of the elements and without considering interaction of the elements, respectively. The mean values of ratios of predicted results P_{S1} and P_{S2} using the proposed method to test results are 0.9166 and 0.9509 with the corresponding coefficient of variation of 0.0483 and 0.0477, respectively. The comparison indicates that the proposed method is conservative and can be used to calculate the ultimate capacity of the compressive columns with holes.

Table 4 Comparison on ultimate capacities between test results and calculated results

| specimens | P_t kN | P_{ABA} kN | P_{C1} kN | P_{C2} kN | P_{S1} kN | P_{S2} /kN | P_N kN | P_{ABA}/P_t | P_{C1}/P_t | P_{C2}/P_t | P_{S1}/P_t | P_{S2}/P_t | P_N/P_t |
|------------|-------------|-----------------|----------------|----------------|----------------|-----------------|-------------|---------------|--------------|--------------|--------------|--------------|-----------|
| AC-11-CH-1 | 157.75 | 57.81 | 59.47 | 61.76 | 52.91 | 54.76 | 53.23 | 1.00 | 1.03 | 1.07 | 0.92 | 0.95 | 0.92 |
| AC-11-CH-2 | 60.3 | 60.83 | 56.39 | 58.68 | 50.30 | 52.14 | 50.95 | 1.01 | 0.94 | 0.97 | 0.83 | 0.86 | 0.84 |
| AC-11-CH-3 | 358.65 | 60.36 | 58.12 | 60.43 | 51.74 | 53.60 | 52.02 | 1.03 | 0.99 | 1.03 | 0.88 | 0.91 | 0.89 |
| AC-11-CH-4 | 457.95 | 58.55 | 56.22 | 58.52 | 50.12 | 51.97 | 50.48 | 1.01 | 0.97 | 1.01 | 0.86 | 0.90 | 0.87 |
| AC-11-CH-5 | 554.05 | 56.41 | 57.05 | 59.36 | 50.87 | 52.72 | 51.45 | 1.04 | 1.06 | 1.10 | 0.94 | 0.98 | 0.95 |
| AC-11-CH-6 | 53.1 | 55.23 | 56.92 | 59.26 | 50.73 | 52.61 | 51.10 | 1.04 | 1.07 | 1.12 | 0.96 | 0.99 | 0.96 |
| AC-21-CH-1 | 55.6 | 58.09 | 55.66 | 58.12 | 49.68 | 51.65 | 49.83 | 1.04 | 1.00 | 1.05 | 0.89 | 0.93 | 0.90 |
| AC-21-CH-2 | 57.4 | 59.75 | 57.55 | 59.80 | 51.26 | 53.07 | 51.72 | 1.04 | 1.00 | 1.04 | 0.89 | 0.92 | 0.90 |
| AC-21-CH-3 | 356.55 | 58.47 | 59.33 | 61.57 | 52.75 | 54.56 | 53.04 | 1.03 | 1.05 | 1.09 | 0.93 | 0.96 | 0.94 |
| AC-21-CH-4 | 457.31 | 57.92 | 57.54 | 59.83 | 51.26 | 53.10 | 51.66 | 1.01 | 1.00 | 1.04 | 0.89 | 0.93 | 0.90 |
| AC-21-CH-5 | 557.65 | 57.88 | 57.44 | 59.89 | 51.28 | 53.25 | 52.03 | 1.00 | 1.00 | 1.04 | 0.89 | 0.92 | 0.90 |
| AC-21-CH-6 | 656.55 | 55.82 | 56.24 | 58.50 | 50.14 | 51.96 | 50.74 | 0.99 | 0.99 | 1.03 | 0.89 | 0.92 | 0.90 |
| AC-12-CH-1 | 54.9 | 53.82 | 57.42 | 59.82 | 51.27 | 53.20 | 52.06 | 0.98 | 1.05 | 1.09 | 0.93 | 0.97 | 0.95 |
| AC-12-CH-2 | 253.65 | 54.92 | 55.76 | 58.21 | 49.76 | 51.73 | 50.02 | 1.02 | 1.04 | 1.08 | 0.93 | 0.96 | 0.93 |
| AC-12-CH-3 | 357.65 | 58.51 | 58.08 | 60.45 | 51.69 | 53.60 | 51.70 | 1.01 | 1.01 | 1.05 | 0.90 | 0.93 | 0.90 |

| | | | | | | | | | | | | | |
|--------------------------|-------|-------|-------|-------|-------|-------|--------|--------|--------|--------|--------|--------|------|
| AC-12-CH-455.55 | 57.38 | 52.99 | 55.52 | 47.50 | 49.52 | 48.18 | 1.03 | 0.95 | 1.00 | 0.86 | 0.89 | 0.87 | |
| AC-12-CH-552.05 | 55.98 | 54.50 | 56.92 | 48.70 | 50.64 | 49.14 | 1.08 | 1.05 | 1.09 | 0.94 | 0.97 | 0.94 | |
| AC-12-CH-6 | 54.9 | 56.08 | 57.69 | 60.08 | 51.42 | 53.34 | 51.75 | 1.02 | 1.05 | 1.09 | 0.94 | 0.97 | 0.94 |
| AC-22-CH-154.00 | 55.33 | 55.20 | 57.61 | 49.31 | 51.24 | 49.85 | 1.02 | 1.02 | 1.07 | 0.91 | 0.95 | 0.92 | |
| AC-22-CH-252.40 | 54.12 | 52.95 | 55.37 | 47.46 | 49.39 | 48.44 | 1.03 | 1.01 | 1.06 | 0.91 | 0.94 | 0.92 | |
| AC-22-CH-354.00 | 55.41 | 56.56 | 58.96 | 50.51 | 52.43 | 51.30 | 1.03 | 1.05 | 1.09 | 0.94 | 0.97 | 0.95 | |
| AC-22-CH-452.05 | 53.12 | 58.68 | 60.91 | 52.21 | 54.00 | 52.60 | 1.02 | 1.13 | 1.17 | 1.00 | 1.04 | 1.01 | |
| AC-22-CH-550.65 | 52.43 | 52.51 | 54.97 | 47.13 | 49.09 | 48.23 | 1.04 | 1.04 | 1.09 | 0.93 | 0.97 | 0.95 | |
| AC-22-CH-649.65 | 50.94 | 58.05 | 60.29 | 51.67 | 53.48 | 52.23 | 1.03 | 1.17 | 1.21 | 1.04 | 1.08 | 1.05 | |
| AC-00-NH-161.03 | 63.01 | 58.18 | 60.45 | 58.18 | 60.45 | 57.98 | 1.03 | 0.95 | 0.99 | 0.95 | 0.99 | 0.95 | |
| AC-00-NH-260.28 | 62.74 | 56.69 | 59.01 | 56.69 | 59.01 | 57.61 | 1.04 | 0.94 | 0.98 | 0.94 | 0.98 | 0.96 | |
| Mean value | | | | | | | 1.0237 | 1.0275 | 1.0702 | 0.9166 | 0.9509 | 0.9258 | |
| Variance | | | | | | | 0.0201 | 0.0504 | 0.0515 | 0.0443 | 0.0453 | 0.0449 | |
| Coefficient of variation | | | | | | | 0.0197 | 0.0490 | 0.0482 | 0.0483 | 0.0477 | 0.0485 | |

Conclusion

The following conclusions can be attained according the experimental and analytical research of 26 axially compressive columns with holes in web. The compressive test results on cold-formed lipped channel sections with holes in the web have shown that the intermediate length columns display the distortional buckling and failure with interaction of local, distortional, and global bending buckling. The circle hole in the web has only a small influence on elastic buckling mode, buckling half-wavelength, and elastic buckling strength of compressive columns. The circle hole in the web can decrease the ultimate load of compressive columns. The reduction increases with the increase of area of the transverse holes. Modifications about the effective width method based on effective width method in current Chinese specification have been proposed. Comparison between predicted results using proposed method and test value demonstrates that the proposed method is well than current Chinese specification. The proposed method provides an accurate and reliable design method for cold-formed steel lipped channel compressive sections with holes. The failure modes and ultimate bending capacity obtained from the FEM analysis are close to test results. This comparison indicates that the finite element model can well analyze the buckling failure mode and ultimate capacity of cold-formed steel compressive members with holes.

Notation

The following symbols are used in this paper:

a_1 、 a_2 = Measure width of the top and bottom lip

| | | |
|---------------|---|--|
| b_1 , b_2 | = | Measure width of the top and bottom flange |
| b | = | Width of element |
| b_c | = | Compressed width of element |
| b_e | = | Effective width of element |
| d | = | Diameter of circle hole |
| E | = | Modulus of elasticity of steel |
| f_y | = | Yield stress |
| h_1 , h_2 | = | Measure width of left and right web |
| k | = | Stability coefficient of the element |
| k_1 | = | Interaction coefficient due to the adjacent element |
| l | = | Length of member |
| P_{ABA} | = | Ultimate capacity analyzed using Finite Element Method |
| P_{C1} | = | Ultimate capacity calculated using Chinese cold-formed steel specification considering interaction of the elements |
| P_{C2} | = | Ultimate capacity calculated using Chinese cold-formed steel specification without considering interaction of the elements |
| P_{crd} | = | Elastic distortional buckling strength |
| P_{crl} | = | Elastic local buckling strength |
| P_N | = | Ultimate capacity calculated using North America cold-formed steel specification |
| P_{s1} | = | Ultimate capacity calculated using proposed method considering interaction of the elements |
| P_{s2} | = | Ultimate capacity calculated using proposed method without considering interaction of the elements |
| P_t | = | Test results |
| P_y | = | Yield strength |
| S_1 | = | Vertical distance of circle holes |
| S_2 | = | Transverse distance of circle holes |
| t | = | Thickness of member |
| α | = | Coefficient |
| ψ | = | Uneven coefficient of the compression stress distribution |
| ρ | = | Calculating coefficient |

Acknowledgements

The author gratefully acknowledges the financial support provided by *National Natural Science Foundation Projects of China* (No: 51308277), *Department of Science and Technology Natural Science Foundation Projects of Jiangxi Province in China* (No: 20151BAB206055), and *China Postdoctoral Science Foundation funded project* (No: 2016M590382). Authors really appreciate Professor Schafer B.W. in Johns Hopkins University and Professor Moen C.D. in Virginia tech who provides the script of ABAQUS for axially-compressive members with holes.

Reference

- Abdel-Rahman N. Cold-formed steel compression members with perforations. Hamilton, Ontario: McMaster University, 1997.
- AISI-S100--2016. *North American specification for the design of cold-formed steel structural members*, 2016.
- Banwait A. S. Axial load behavior of thin-walled steel sections with openings. Hamilton, Ontario: McMaster University, 1987.
- GB50018-2002. *Technical code of cold-formed thin-wall steel structures*, 2002. (In Chinese)
- GB/T228.1-2010. *Metallic materials--Tensile testing--Part 1: Method of test at room temperature*, 2010. (In Chinese)
- He Baokang, Zhou Tianhua. Local buckling of cold-formed steel sections and a unified approach for calculating effective width in AISI specification, *Progressing Steel Building Structures*, 2005, 7(4): 6-10. (In Chinese)
- Loove R. Local buckling capacity of C-shaped cold-formed steel sections with punched webs. *Canada Journal Civil Engineering*, 1984, 11(1): 1-7.
- Moen C.D. Direct strength design for cold-formed steel members with perforations, MD, Baltimore: Johns Hopkins University, 2008.
- Moen,C.D., Schafer, B.W. Elastic buckling of cold-formed steel columns and beams with holes. *Engineering Structure*, 2009a, 31(12): 2812-2824.
- Moen,C.D., Schafer, B.W. Elastic buckling of thin plates with holes in compression or bending. *Thin-walled Structures*, 2009b, 47:1597-1607.
- Moen, C.D., Schafer, B.W. Experiments on cold-formed steel columns with holes. *Thin-walled Structures*, 2008, 46:1164-1182.
- Moen, C.D., Schafer, B.W. Direct strength method for design of cold-formed steel columns with holes. *Journal of Structural Engineering*, ASCE.2011, 137(5):559-570.
- Ortiz-Colberg R. A. The load carrying capacity of perforated cold-formed steel columns, Ithaca, NY: Cornell University, 1981.
- Pu Y., Godley M.H.R., Beale R.G., et al. Prediction of ultimate capacity of perforated lipped channels. *Journal Structure Engineering-ASCE*, 1999,125(5):510-514.
- Rhodes J, Schneider F. D.(1994). The compression behavior of perforated elements, *Twelfth international specialty conference on cold-formed steel structures: recent research and developments in cold-formed steel design and construction*. Saint Louis: University of Missouri-Rolla, 1994: 11-28.
- Sivakumaran K. S. Load capacity of uniformly compressed cold-formed steel section with punched web. *Canada Journal Civil Engineering*, 1987,14(4):550-558.
- Wen Shuangling. Flexural-torsional buckling of axially loaded columns with perforated cold formed thin-walled section. *Journal of Civil Engineering*, 1996, 29(1): 72-79. (In Chinese)
- Zhou Jinjiang, Yu Shaofeng. Equivalent calculation of buckling stress for cold-formed thin wall perforated channel column. *Steel Construction*, 2010, 25(2): 27-31. (In Chinese)